Polymer Chemistry

PAPER

View Article Online
View Journal | View Issue

Cite this: *Polym. Chem.*, 2019, **10**, 5920

First phosphorus AB_2 monomer for flame-retardant hyperbranched polyphosphoesters: AB_2 *vs.* $A_2 + B_3$†

Jens C. Markwart, ‡[a,b] Alexander Battig, ‡[c] Thomas Kuckhoff,[a] Bernhard Schartel *[c] and Frederik R. Wurm *[a]

Received 1st August 2019,
Accepted 24th September 2019

DOI: 10.1039/c9py01156k

rsc.li/polymers

Branched polymers are an important class of polymers with a high number of terminal groups, lower viscosity compared to their linear analogs and higher miscibility, which makes them especially interesting for flame retardant applications, where the flame retardants (FR) are blended with another polymer matrix. Hyperbranched polyphosphoesters (*hb*PPEs) are gaining more and more interest in the field of flame retardancy, as low molar mass FRs often have the disadvantage of blooming out or leaching, which is not desired in consumer products. Here, we present the first phosphorus-based AB_2 monomer for the synthesis of *hb*PPEs and assess its flame-retardant performance in an epoxy resin compared to a *hb*PPE synthesized by an $A_2 + B_3$ approach. The *hb*PPE synthesized from an AB_2 monomer exhibited a slightly higher performance compared to a similar *hb*PPE, which was prepared by $A_2 + B_3$ polyaddition, probably due to its higher phosphorus content.

Introduction

Hyperbranched (*hb*) polymers, with their high number of terminal groups, lower viscosity, and higher matrix miscibility compared to their linear analogs, are especially interesting as flame-retardant additives, as effective blending with a polymer matrix is essential.[1–5] Moreover, flame retardants (FRs) with complex architectures have a decreased impact on the material properties of polymers.[6,7]

The synthesis of such dendritic polymers can be achieved by multi-step dendrimer syntheses, which are time-consuming, often need several purification steps and therefore unattractive for large scale, flame-retardant applications.[1,8] In contrast, *hb* polymers are readily available by one polymerization step, *e.g.* by polycondensation of commercially available $A_2 + B_3$ monomer mixtures. *hb* polymers do not exhibit an architecture as perfect as dendrimers, because the polymers are statistically branched with structural and molar mass dispersities. Despite these architectural differences, *hb* polymers still retain many of the particular properties of dendrimers.[1,3]

Here, we present, to the best of our knowledge, the first phosphorus-based AB_2 monomer for the synthesis of *hb* polyphosphoesters (*hb*PPEs), which are promising candidates as halogen-free flame-retardant additives.

To date, *hb*PPEs were synthesized by $A_2 + B_3$ approaches or by using AB* inimers, for which representative examples are given in Scheme 1. Penczek *et al.* prepared a family of oligomers with acidic end groups by an $A_2 + B_3$ approach by addition of H_3PO_4 to a bisphenol A based epoxy resins.[9] Liu *et al.* described a water-soluble *hb*PPE through a self-condensing ring-opening polymerization of an AB* inimer (2-(2-hydroxyethoxy)ethoxy-2-oxo-1,3,2-dioxaphospholane).[10] More recently, we used radical polyaddition of phosphorus-based B_3-monomers with dithiols to prepare *hb*PPEs, polyphosphoramidates, and -amides to elucidate their decomposition mechanism as flame-retardant additives in epoxy resins.[11]

Previous studies used *hb*PPEs due to their biocompatibility and biodegradability for mostly biomedical[12,13] or optical applications.[14] With the ban of some halogenated FRs, phosphorus-based derivatives as effective alternatives are in growing demand in recent years.[15–18] Moreover, polymeric FRs are interesting as they exhibit less blooming out or leaching compared to low molar mass FRs, which is not desired in consumer products.[19] In addition, the thermal stability of low molar mass FRs is usually lower, thus limiting their processability. In comparison, oligomeric or polymeric FRs exhibit

[a]*Physical Chemistry of Polymers, Max Planck Institute for Polymer Research, Ackermannweg 10, 55128 Mainz, Germany. E-mail: wurm@mpip-mainz.mpg.de*
[b]*Graduate School Materials Science in Mainz, Staudinger Weg 9, 55128 Mainz, Germany*
[c]*Bundesanstalt für Materialforschung und -prüfung (BAM), Unter den Eichen 87, 12205 Berlin, Germany*

†Electronic supplementary information (ESI) available. See DOI: 10.1039/C9PY01156K

‡These authors contributed equally to this work.

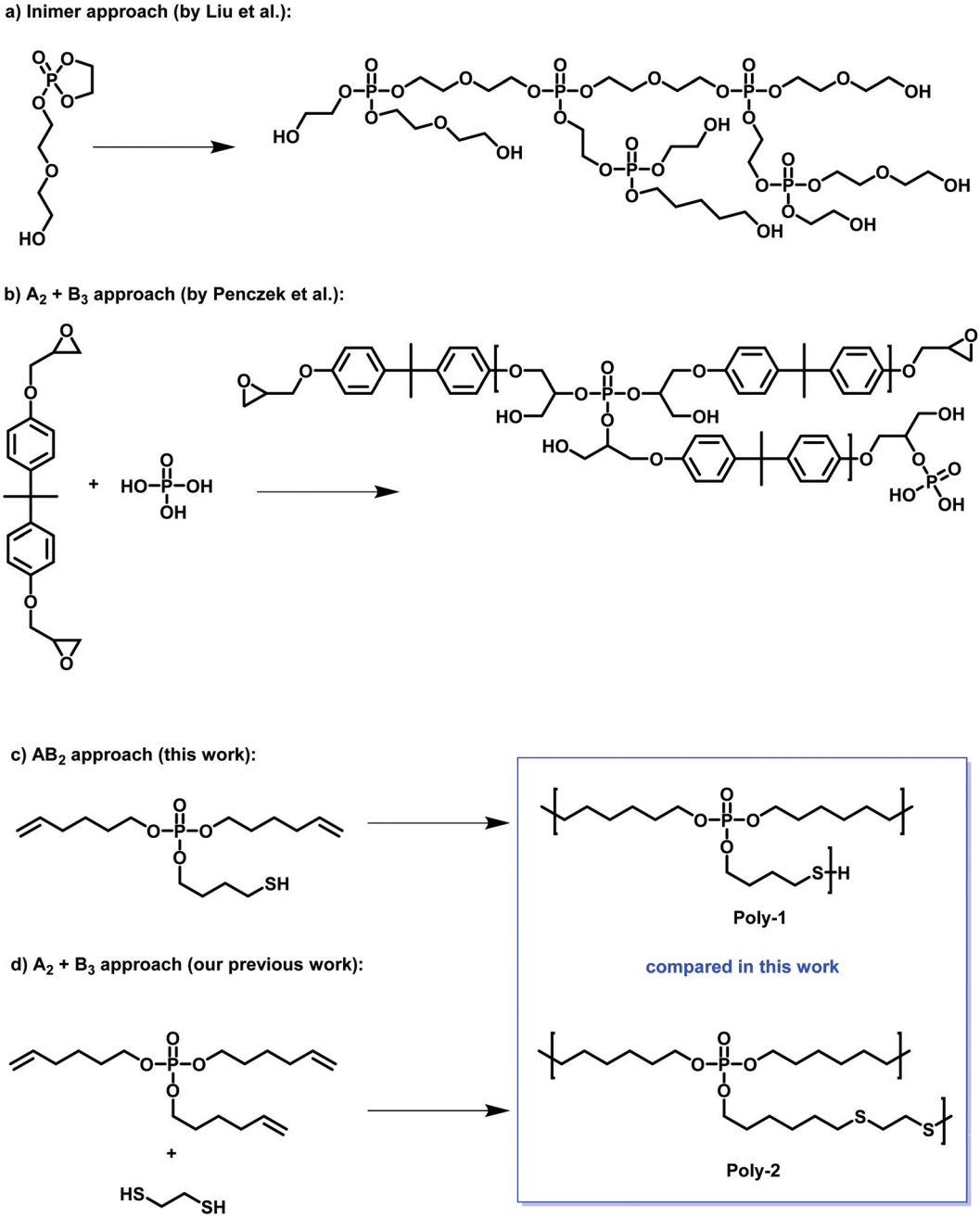

Scheme 1 Examples of *hb*PPEs in literature: (a) *hb*PPEs *via* inimer approach by Yan *et al.*[10] (b) A_2 + B_3 approach by Penczek *et al.*[9] (c) this work: AB_2 monomer and (d) the comparison A_2 + B_3 approach by Battig *et al.*[11]

increased thermal stability and therefore higher effectiveness, which leads to improved chemical interaction during decomposition, yielding higher char yields and better overall flame retardancy.[11,20,21] Furthermore, FRs with different architectures have been investigated, stressing the impact of complex chemical structure on the mechanical properties and glass-transition temperature (T_g) of the polymer matrix.

With the first example of an AB_2-type phosphate monomer for radical polycondensation, we present a straightforward approach to *hb*PPEs and thus avoid the chance of cross-linking during the synthesis. In addition, the versatile monomer design, which was exemplarily used for **1**, allows further tuning of the P-content or the hydrophilicity, *i.e.* matrix compatibility, by variation of the alkyl-spacers, which makes the herein presented approach also applicable for other polymer matrices.

Results and discussion

For the synthesis of hyperbranched (*hb*) polymers, two common approaches exist: The AB_n and A_n + B_m approach.[22] In

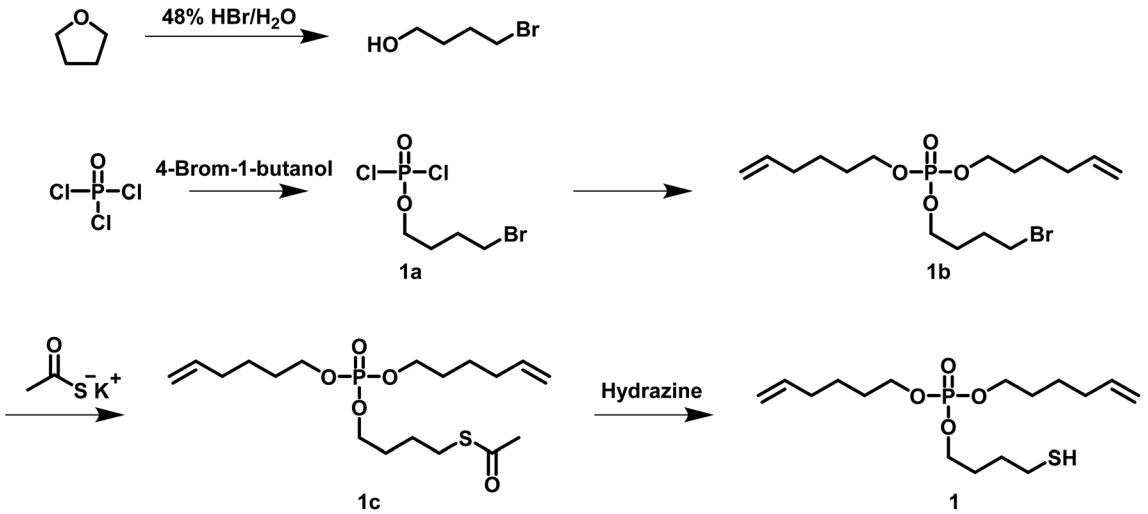

Scheme 2 Synthesis scheme of di(hex-5-en-1-yl)(4-mercaptobutyl)phosphate (**1**).

the AB_n approach, first envisioned by Flory in 1952, only a single monomer with an AB_n ($n \geq 2$) structure is used.[23] When A and B groups react selectively with each other, a statistically branched polymer without cross-linking is generated.[24]

In the A_n + B_m approach, two monomers are used for polymerization (A_n and B_m (n, $m \geq 2$)), with the most common method being the A_2 + B_3 approach, as several monomers are commercialized. However, to obtain soluble polymers, the polymerization needs to be terminated before the gel point, which requires adjustment of the reaction conditions, or adjustment of the monomer feed-ratio, *etc*. for each monomer set.[24–26]

For the synthesis of a *hb* polyphosphoester (*hb*PPE) *via* the AB_n approach, an AB_2 phosphoester with two different reactive groups (A and B) was prepared: di(hex-5-en-1-yl)(4-mercaptobutyl)phosphate (**1**) was synthesized in a four step reaction, starting from $POCl_3$ and 4-bromobutan-1-ol (Scheme 2). 4-Bromobutan-1-ol was obtained from refluxing THF with HBr for several hours, followed by neutralizing with $NaHCO_3$ and extraction with DCM, according to a literature protocol.[27] An excess $POCl_3$ was reacted with 4-bromobutan-1-ol. Removing the excessive amount of $POCl_3$ gives compound **1a**. **1a** was used in the next step without further purification and treated with 5-hexen-1-ol to give compound **1b**. The electrophilic alkyl bromide in **1b** renders it a versatile precursor for various modifications like the introduction of other functional groups or as a monomer for ADMET itself. **1b** was mixed with potassium thioacetate and stirred overnight to obtain compound **1c**, which was purified by solvent extraction. The final AB_2-monomer **1** for radical polyaddition was obtained after treating **1c** with hydrazine, which cleaved the thioacetate group and released the free thiol. Monomer **1** is a liquid at room temperature and has a phosphorus content of 8.84 wt%. It is soluble in most organic solvents (*e.g.* toluene, tetrahydrofuran, ethyl acetate, acetone, dichloromethane and chloroform), but insoluble in water. It is important to mention that the butyl spacer between thiol and phosphorus is essential for the monomer stability: a similar monomer structure with an ethyl spacer was recently used to prepare linear PPEs with pendant 2-acetylthioethyl side chains.[28] In this case, the pendant group acted as a protective group for the P-OH group after treatment with hydrazine, followed by a 3-*exo-tet* mechanism to release the P-OH group after cleavage of the phosphoester.

^{1}H NMR spectroscopy (Fig. 1a) of **1** revealed two distinct resonances at 2.60 ppm (methylene group next to the thiol) and 1.36 ppm (SH). The olefinic signals were detected as multiplets in the region of 5.80 ppm and 5.00 ppm. The methylene group next to the double bond was found at 2.09 ppm and the methylene group next to the P–O group had a resonance at 4.05 ppm. The remaining signals of the methylene units were detected between 1.81 ppm and 1.45 ppm. The ^{31}P NMR spectrum shows a single signal at −0.68 ppm (Fig. 1c).

Compound **1** was used as AB_2 monomer for the radical thiol–ene polyaddition to produce *hb* **poly-1** (Scheme 3). The statistically branched polymer with dendritic (D), linear (L), and terminal (T) units (*cf.* Scheme 3) was obtained as a viscous oil with a T_g of *ca.* −88 °C (Fig. 1i). The ^{1}H NMR pattern of **poly-1** was very similar to that of **1** (Fig. 1b); however, with increasing degree of polymerization, the olefinic resonances, the methylene group next to the S–H group and the S–H signal decreased. Due to signal overlap, calculation of a degree of branching was not possible. The polymerization was followed by GPC and NMR by taking samples throughout the reaction and calculating the ratio between the methylene groups next to the P–O (n_{Ester}) and the double bond ($n_{\text{Double-bond}}$) $n_{\text{Double-bond}}/n_{\text{Ester}}$ (marked blue in Fig. 1f). During polymerization, a new resonance appeared at 2.54 ppm representing the methylene groups next to the thioethers. Polymerization was conducted at different temperatures (50 °C, 70 °C, and 90 °C) with 0.03 eq. AIBN and additionally with different amounts of AIBN (0.03 eq., 0.06 eq. and 0.09 eq.) at 70 °C (*e.g.* Fig. 1h).

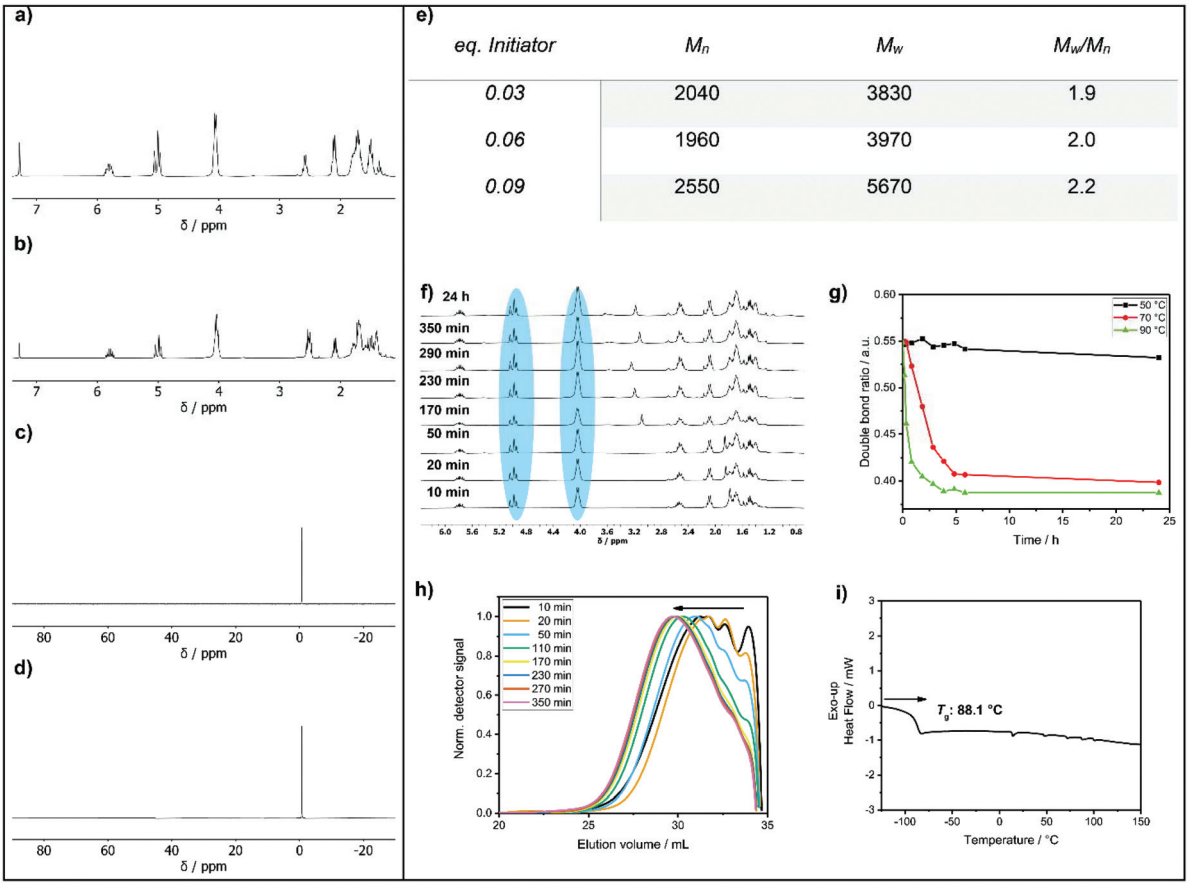

Fig. 1 ^{1}H NMR spectra of **1** (a) and **poly-1** (b); ^{31}P NMR spectra of **1** (c) and **poly-1** (d). (e) Molar masses of the polymer at different initiator equivalents; (f) ^{1}H NMR kinetic of the polymerization of **1** at 90 °C and 0.03 eq. AIBN. (g) Polymerization kinetics measured by NMR (change of $n_{\text{Double-bond}}/n_{\text{Ester}}$ over time) at different temperatures (50 °C, 70 °C and 90 °C). (h) GPC kinetics of the polymerization of **1** with 0.09 eq. AIBN (measured in DMF). (i) Differential scanning calorimetry (DSC) of **poly-1** with a T_g at 88.1 °C.

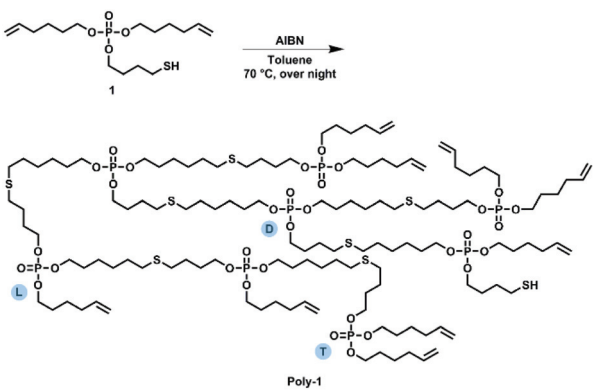

Scheme 3 Hyperbranching polymerization of monomer **1** to **poly-1** by radical thiol–ene polyaddition.

From the NMR data, only very slow reaction kinetics were detected at 50 °C, while at elevated temperatures (70 °C), no further reaction was observed after 7 h (Fig. 1g). With increasing initiator concentration, a slight increase in molar mass was observed (Fig. 1e). The ^{31}P NMR resonance of **poly-1** remained relatively unchanged compared to the monomer with a single signal at −0.70 ppm (Fig. 1d). As the degree of polymerization increased, $n_{\text{Double-bond}}/n_{\text{Ester}}$ became smaller.

For the flame retardancy investigations, the resulting polymer had an M_w of 5500 g mol^{-1} with an M_w/M_n of 2.39 (GPC in DMF). **Poly-1** was used as an additive flame retardant (FR) in epoxy resins, and the FR properties were compared to a similar *hb*PPE prepared by the $A_2 + B_3$ approach (**poly-2**, Scheme 1), M_w of 11 300 g mol^{-1} with an M_w/M_n of 3.29 (GPC in THF),[11] and a commercial phosphate-based FR, namely bisphenol A bis(diphenyl phosphate) (**BDP**), which was already used in epoxy resins like DGEBA/DMC.[19,29] The ratio $n_{\text{Double-bond}}/n_{\text{Ester}}$, an indication of the amount of terminal double bonds, was identical for **poly-1** and **poly-2** (0.39). Looking at the phosphorus content, **poly-1** exhibits the same amount of P when compared to the monomer. In contrast, for **poly-2** the P content varied, depending on the monomer ratio and workup procedure. The theoretical phosphorus content deviated from the measured phosphorus content after precipitation. The theoretical phosphorus content of **poly-2** is 5.1 wt%, the measured phosphorus content by elemental analysis is 7.7 wt%.

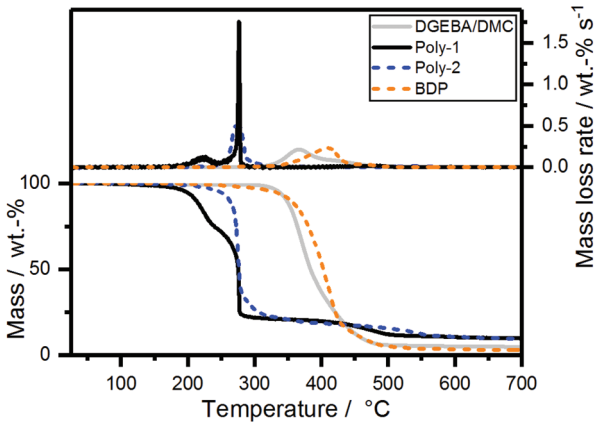

Fig. 2 Mass loss (bottom) and mass loss rate (top) over T of **poly-1**, **poly-2**, bisphenol A bis(diphenyl phosphate) and neat epoxy resin from TGA measurements (10 K min^{-1}; N_2).

Pyrolysis: thermal decomposition of FRs *via* TGA

The pyrolytic decomposition of the FRs was investigated using thermogravimetric analysis (TGA) (Fig. 2). During burning, the thermal decomposition of the material feeds volatile fuel into the flame zone, where exothermal combustion reactions, *i.e.* oxidation, occur. However, at the solid/gas interface, the reactions in the anaerobic pyrolysis zone determine the fire behavior. This model is accurate for polymeric materials in developing fires, which are simulated in the cone calorimeter, but also reaction-to-small-flame tests such as UL94 and LOI. Therefore, investigations into the pyrolytic reactions of FRs and FR-containing polymers *via* TGA in nitrogen atmosphere are an important analytical tool to understand the chemical mechanisms underlying the FR's modes of action.[30]

The mass loss curve of **poly-2** exhibited a main single decomposition step at 274 °C with a gradual decomposition thereafter (Fig. 2). **Poly-1** exhibited an additional decomposition step at *ca.* 226 °C, followed by the second decomposition step at the same temperature as **poly-2**. The additional decomposition step might be rationalized with the cleavage of the terminal alkyl-SH group, similar to the mechanism described previously by Markwart *et al.*,[28] which was confirmed by the presence of tetrahydrothiophene (from pyrolysis-(Py)-GC/MS measurements at 250 °C (Fig. S6 and S8†) and TGA-FTIR measurements (Fig. S16†)). The amount of residue at 700 °C was very similar for both polymers (**poly-1**: 9.7 wt%, **poly-2**: 9.3 wt%).

Pyrolysis: evolved gas analysis of FRs *via* TG-FTIR

Evolved gas analysis during pyrolysis of **poly-1** was performed *via* Py-GC/MS and TG-FTIR measurements. The analysis of epoxy resin (EP) and **poly-2** has been previously described in detail and will therefore not be discussed herein.[11,31] For **poly-1**, two single-shot Py-GC/MS measurements at varied pyrolysis temperatures (250 °C and 500 °C) were conducted to isolate the decomposition products in the first decomposition step. The gas chromatogram at 250 °C (Fig. S6†) displays a single large signal at 5.62 min retention time, while at 500 °C (Fig. S7†), additional signals between 2.60–3.56 min were detected, as well as minor signals >5.62 min. The mass spectrum at 5.62 min was identified as tetrahydro thiophene (Fig. S8 and S9†), thus confirming the cleavage of alkyl-SH groups of **poly-1** during the first decomposition step seen in TGA. The signals between 2.60–3.56 min corresponded to 1,5-hexadiene (Fig. S10 and S11†) and its thermal rearrangement products. The rearrangement is proven by the presence of cyclohexane (Fig. S12 and S13†) at 3.56 min, a product of cyclization of 1,5-hexadiene. At 6.57 min, the signal was identified as 5-hexen-1-ol (Fig. S14 and S15†) resulting from hydrolysis of the phosphate-moiety.

Pyrolysis: EP-FR preparation and material properties

The FR-performances of **BDP**, **poly-1**, and **poly-2** were studied in an epoxy resin (**EP**) based on bisphenol A diglycidylether (DGEBA) and 2,2′-dimethyl-4,4′-methylene-bis-(cyclohexylamine) (DMC). All epoxy plates were prepared in the following manner: DGEBA was mixed with the respective FR (loading: 10 wt%) until homogenous. Then, DMC was added, and the mixture was poured into appropriately sized aluminum molds, followed by curing for 30 min at 90 °C, 30 min at 120 °C, and 1 h at 150 °C. Additive FRs can act as plasticizers in epoxy resins, thus reducing the glass transition temperature (T_g) of the resulting composite. Differential scanning calorimetry (DSC) measurements revealed that the flame retardant containing epoxy resins (**EP-FRs**) lowered T_g by an average of 24 °C: **Poly-1** had the strongest impact on the T_g of **EP**, lowering it by about 30 °C to 124 °C ($T_{g,\ EP}$ = 155 °C), while **poly-2** and **BDP** had a similar impact on the T_g of EP ($T_{g,\ EP\text{-}poly2}$ = 132 °C; $T_{g,\ EP\text{-}BDP}$ = 133 °C). The impact of FRs on the T_g of EP is presented in Fig. S20,† and the change of T_g relative to **EP** is noted.

Pyrolysis: thermal decomposition and evolved gas analysis of EP-FRs *via* TGA and TG-FTIR

The decomposition behavior of **EP-FRs** was investigated by analyzing the mass loss and evolved gas during pyrolytic decomposition *via* TGA coupled with FTIR (Table S2†). A significant change in decomposition behavior was observable for all **EP-FRs**, as the mass loss and mass loss rate curves (Fig. 3) and the change in residue yields at 700 °C proved. The pure epoxy decomposed with an onset temperature ($T_{5\%}$) of 338 °C and reached the temperature of maximum mass loss rate (T_{max}) at 372 °C. EP decomposed in a single main step with a mass loss equal to 62 wt%. Following the main decomposition step, a shoulder beginning at 424 °C with a mass loss of 33 wt% was observed. At 700 °C, the residue yield was 4.5 wt%. The mass loss and evolved gas analysis of the epoxy resin (DGEBA/DMC) has been extensively investigated; therefore, it will not be discussed further.[32,33] When **BDP** was added to the resin (**EP-BDP**), the composite decomposed similarly to the pure **EP**, but $T_{5\%}$ was lowered by about 33 °C, and T_{max} was 15 °C lower than **EP**. This change is attributed to a reduction in cross-linking density of the **EP**-system when additives are present.[34] The plateau which started at 423 °C exhibited a

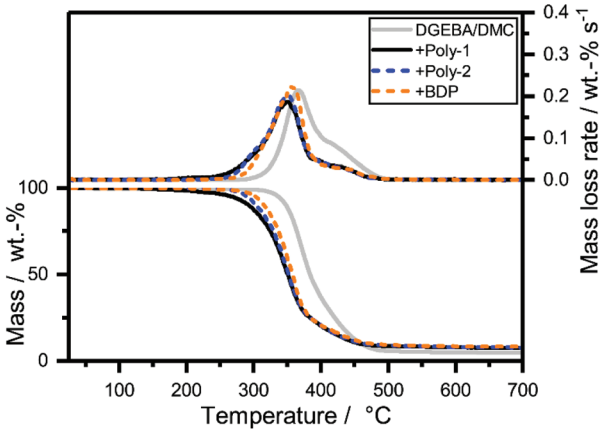

Fig. 3 Mass loss (bottom) and mass loss rate (top) over T of EP-FRs from TGA measurements (10 K min^{-1}; N_2).

lower decomposition rate compared to pure **EP**. An increase in mass loss at T_{max} to 75 wt% and a decrease to 16 wt% at the shoulder was observable. An explanation for this phenomenon is the interaction of the FR with the decomposing matrix.[35] More specifically, the phenol-derivates and cycloalkanes are bound; these exhibit a production rate maximum in this temperature range.[36] As a result, the residue yield of **EP-BDP** increased to 8.1 wt%, which is nearly twice that of pure EP.

All *hb*-FR containing EPs (**EP-*hb*-FRs**) exhibited a decomposition behavior similar to **EP-BDP**. The $T_{5\%}$ of **EP** was lowered by 70 °C for **poly-1** and 47 °C for **poly-2**. T_{max} was also lowered when FRs were present, on average by approx. 16 °C. The lower $T_{5\%}$ of **EP-poly-1** compared to **EP-poly-2** is caused by the additional decomposition step in **poly-1**. All residue yields of **EP-FRs** were in a similar range, and all investigated FRs increased the residue of **EP** (7.9 and 7.7 wt% for **poly-1** and **poly-2**, respectively, and 8.1 wt% for **BDP**). The neat **EP** had a residue yield of only 4.6 wt%. This increase in residue indicates that the tested FRs interact with the decomposing matrix. As a result, thermally stable residues are formed.

From the evolved gas analysis of **EP-FRs** *via* TG-FTIR (Fig. S17†), two distinct decomposition products were visible for **EP-poly-1** and **EP-poly-2**, the first appearing in the range of about 290 °C and the second between 360–380 °C. At *ca.* 290 °C, the spectra of **EP-poly-1** and **EP-poly-2** exhibited the evolution of 5-hexen-1-ol, a product of either hydrolysis or transesterification. Its presence indicates that *hb*-FRs are active near $T_{5\%}$, forming either lower molecular phosphates (hydrolysis) which are active in the condensed phase, or phosphorylating the polymer matrix (transesterification), thus forming char precursors. The condensed phase mode of action is additionally proven by hot-stage FTIR (Fig. S19†). At 360–380 °C, all spectra are identical to EP, as the matrix decomposes in this temperature range.

Pyrolysis: condensed phase analysis of EP-FRs *via* hot-stage FTIR

The condensed phase mode of action of **poly-1** and **poly-2** in **EP** was proven by hot-stage FTIR measurements (Fig. S18 and S19†). Fig. S18† displays the unique signals of **EP-poly-1** at 300 °C, namely 1146 and 1108 cm^{-1}, which are shifted to slightly lower wavenumbers and increase in intensity at 500 °C (Fig. S19†). These signals may correspond to ν(P═O) of R_2–(P═O)–OH resulting from the cleavage of terminal alkyl-SH groups which occurs more readily than cleavage of terminal hexene-moieties, as observed in Py-GC/MS (Fig. S8†) and TG-FTIR measurements (Fig. S16†) of **poly-1**. It is conceivable that **poly-1** is more reactive than **poly-2** in terms of phosphorylation of the epoxy resin matrix, especially given the increase in residue yields of fire testing and pyrolysis (Tables S1 and S2,† respectively). At 600 °C, the hot-stage FTIR spectrum of **EP-poly-1** exhibits many bands that are also present in **EP-poly-2** and **EP-BDP**, which have already been previously described as phosphorus signals.[11] Moreover, additional bands at 1400, 1125, 1010, 974, and 585 cm^{-1} are present. Many types of compounds, including vinylene-moieties, cyclic aliphatic hydrocarbons, and secondary or tertiary alcohols, present signals at these wavenumbers. While the identification of specific compounds in hot-stage FTIR is not always possible, it is certain that the spectrum of **EP-poly-1** presents clear signals that are distinct and different from **EP**, thereby proving a condensed-phase spectrum of **poly-1** in **EP**.

Fire testing: forced flaming conditions

All **EP-*hb*-FRs** reduced the fire load (THE) of EP. **Poly-1** decreased the fire load of **EP** by 21%, whereas **poly-2** decreased the fire load by 17% and **BDP** by 19%. **Poly-1** reduced THE of **EP** more strongly than **poly-2** because it was able to retain more fuel in the condensed phase, as evidenced by its higher residue yield (Fig. 4d). This fuel retention may be caused by the higher reactivity of **poly-1** compared to **poly-2**: as **poly-1** has a lower $T_{5\%}$, its decomposition products may interact earlier with the decomposing matrix than **poly-2**, therefore increasing char yield, *i.e.* fuel fixation, and thus lowering THE. The tested FRs lowered the peak of heat release rate (PHRR) of **EP** by *ca.* 30% for **BDP** and **poly-1**, and by 44% for **poly-2**. The HRR curves (Fig. 4a) indicate that the formation of a protective char layer on the sample surface resulted in a plateau-like shape approx. 30 s after ignition, reducing PHRR by shielding the underlying material from irradiation. All FRs increased residue yields in the order **EP-poly-1** > **EP-poly-2** > **EP-BDP**. **EP-Poly-1** exhibited the highest residue amount (11.5 wt%) and **EP-BDP** showed the lowest (3.1 wt%). The residues after fire testing (Fig. 4d) help visualize the differences in fire performance of **poly-1** and **poly-2** in EP: The residue of **EP-poly-2** was more voluminous than that of **EP-poly-1**, pointing to higher gas emission, similar to intumescent FR systems. This large char volume was effective in shielding some of the underlying material, acting as a protective layer and thereby reducing PHRR of EP.[37] However, **EP-poly-1** exhibited a lower THE and higher residue yield than **EP-poly-2**, because the thermal properties of its char were greater. As a result, **poly-1** was better able to bind fuel in the condensed phase in the form of char, which increased residue yields and thus reduced the fire load, *i.e.* THE. Although EHC of both materials were nearly

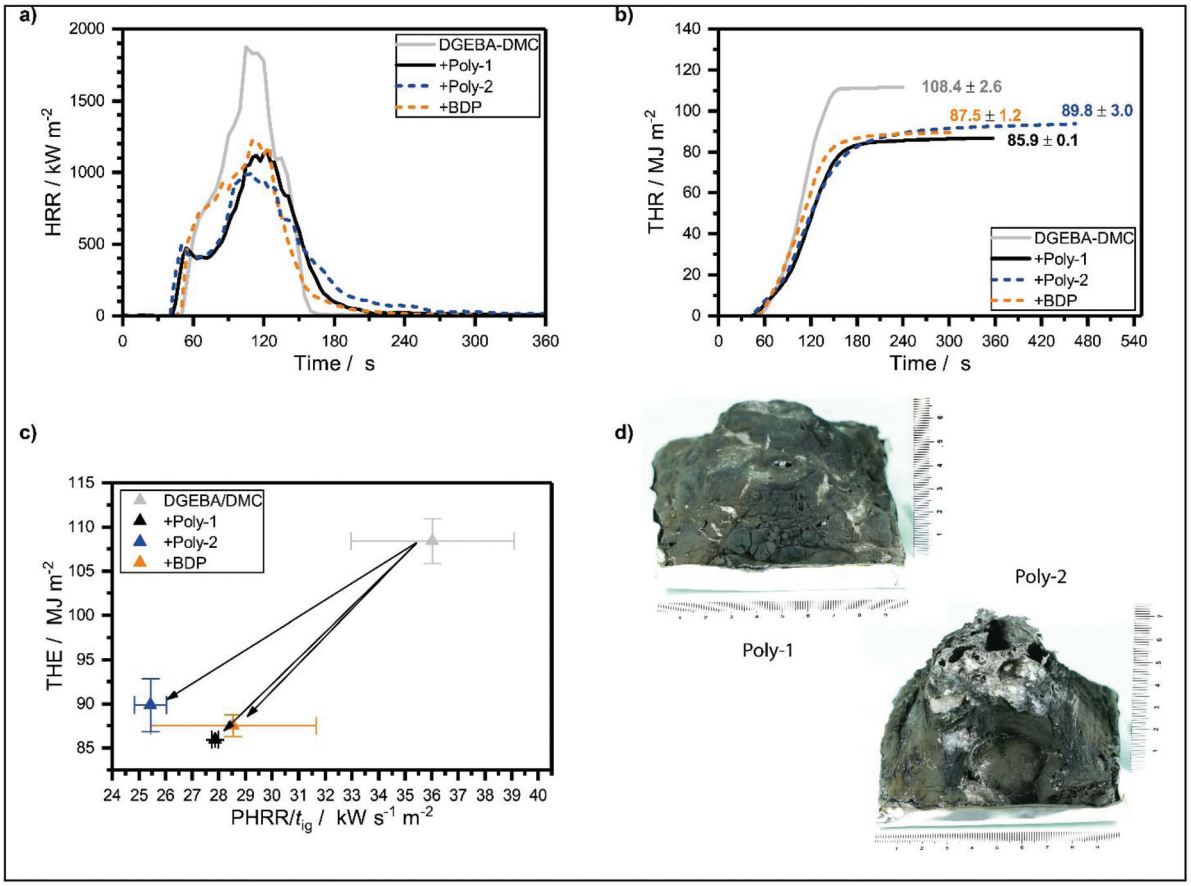

Fig. 4 (a) Heat release rate (HRR) of epoxy resin and epoxy resin with FRs. (b) Total heat released (THR) of epoxy resin and epoxy resin with FRs. (c) Petrella plot of the different epoxy resins with all FRs having a positive effect (lowering THE and PHRR/t_{ig}). (d) Char residues of **EP-poly-1** and **EP-poly-2** after cone calorimeter test. Residue of **EP-poly-2** is more voluminous than that of **EP-poly-1**, pointing to higher gas emission, similar to intumescent FR systems.

identical, the change in char characteristics explains the difference in fire performance, as the residue morphology and its properties often determine effective flame retardancy.[35]

Additionally, the effective heat of combustion (EHC) was reduced by the release of P-containing volatiles. These P-containing volatiles acted in the gas phase as radical scavengers, *i.e.* by lowering the concentration of highly reactive radicals (H$^{\bullet}$, HO$^{\bullet}$, CO$^{\bullet}$, *etc.*) through P$^{\bullet}$ or PO$^{\bullet}$ radicals. The resulting flame inhibition led to less complete combustion; additionally, P enhanced charring thus stored fuel in the condensed phase, all of which resulted in a reduction of THE (Fig. 4b).

To further assess fire behavior and flame retardancy, the fire load (THE) is often plotted against the fire growth index (PHRR/t_{ig}, Fig. 4c),[38] because THE describes heat release quantitatively, however it does not describe the release rate. PHRR/t_{ig} is a means of describing the time-dependent flashover potential or fire growth index, *i.e.* the severity of a fire, or peak heat release potential; however, it is not quantitative. The investigated FRs reduced both PHRR/t_{ig} and THE of **EP**, which had a PHRR/t_{ig} of 36 kW m^{-2} s^{-1} and a THE of 110 MJ m^{-2}. **EP-Poly-1** had a performance similar to **EP-BDP**: BDP reduced THE of **EP** by 19% to 88 MJ m^{-2} and **poly-1** reduced it by 21% to 86 MJ m^{-2}. The PHRR/t_{ig} was reduced by 21% to 29 kW s^{-1} m^{-2} and by 23% to 28 kW s^{-1} m^{-2} for **BDP** and **poly-1**, respectively. **Poly-2** exhibits a higher THE compared to **poly-1** and BDP but has a stronger reduction in PHRR/t_{ig}. The graph visualizes the overall good flame-retardancy potential of the *hb*-FRs: a shift to the lower-left corner of the coordinate system indicates a reduction of overall heat and fire growth. Both *hb*-FRs lower both values on a similar level to the benchmark material, proving their efficacy for this polymer resin system. Moreover, **poly-1** exhibited lower fire loads than **poly-2** in **EP**; this implies that **poly-1** was more able to bind fuel in the condensed phase, as proven by the higher overall char yield. On the other hand, **poly-2** reduced the fire growth rate more strongly than **poly-1** in **EP**: this resulted from the better thermal barrier properties of **EP-poly-2**'s char, which lowered PHRR, as well as the higher thermal stability of **poly-2** which led to an increased t_{ig}.

Conclusion

Hyperbranched polymers, especially polyphosphoesters, are interesting candidates as polymeric flame retardants. *hb*PPEs

were previously prepared by $A_n + B_m$ approaches, which might result in cross-linked PPEs, as adjustment of the monomer feed-ratio or termination before the gel point needs to be carefully conducted. Herein, we presented the first phosphorus-based AB_2 monomer (**1**), allowing the synthesis of *hb*PPEs in a single polyaddition step without the chance of undesired cross-linking.

In addition to the simplified polymerization procedure, **poly-1** exhibited a slightly higher performance compared to similar *hb*PPEs (**poly-2**), prepared by $A_2 + B_3$ polyaddition, probably due to its higher phosphorus content. This work further extends the possibilities for the preparation of branched polyphosphoesters, which might be used in biofriendly flame retardant applications or biomedical applications.

Experimental section

Materials

All chemicals were purchased from commercial suppliers as reagent grade and used without further purification.

Samples for TGA-FTIR and hot-stage FTIR were milled prior to use. Powdered specimens were obtained using a RETSCH CryoMill under liquid nitrogen cooling.

DSC

For Differential Scanning Calorimetry (DSC), a Mettler Toledo DSC 823^e was used. With a heating and cooling rate of 10 K min^{-1}, three measurements of heating, cooling and heating were performed. The measurements were done in a nitrogen atmosphere with a flow rate of 30 mL min^{-1}.

EP-FRs were measured on a Netzsch 204 F1, type Pheonix. Two cooling and three heating runs were performed on 5 mg bulk material samples; the rate was 10 K min^{-1}, the temperature range was −80 to 180 °C, and the nitrogen flow rate was 30 mL min^{-1}. The second and third heating rate were used to determine T_g.

TGA

For the thermogravimetric analysis (TGA) of the neat flame retardants, a Mettler Toledo TGA/DSC 3+ in a nitrogen atmosphere was used. Using 10 mg of the sample, the measurements were performed in a range from 25 °C to 700 °C with a heating rate of 10 K min^{-1}.

TG-FTIR

Pyrolysis investigations into mass loss and evolved gas analysis were performed *via* thermogravimetric analysis (TGA) on a Netzsch TG 209, type Iris, which was coupled *via* transfer line to a Bruker Tensor 27 infrared spectrometer (FTIR). For TG-FTIR measurements of EP and EP-FRs, 10 mg powdered samples were used, while for pure *hb*-FRs, 5 mg samples were measured. Measurements were conducted from 30–900 °C (10 K min^{-1}) under a 30 ml min^{-1} nitrogen purge. Evolved gases passed through a transfer line heated to 270 °C into the FTIR gas cell which was also heated to 270 °C. The measuring range was 4000–400 cm^{-1} with a resolution of 1 cm^{-1}.

Hot stage FTIR

Pyrolysis investigations of the condensed phase activity were performed on a Bruker Vertex 70 FTIR equipped with a Linkam FTIR600 hot stage cell. Powdered EP and EP-FR samples (*ca.* 5 mg) were mixed with 150 mg KBr in a mortar and pestle, then pressed into a platelet at 7 bar. Specimens were heated from 30–600 °C at a rate of 10 K min^{-1} under a nitrogen atmosphere. The measuring range was 4000–400 cm^{-1} with a resolution of 0.4 cm^{-1}.

Pyrolysis-gas chromatography-mass spectrometry (Py-GC/MS)

Pyrolytic evolved gas analysis was performed on a pyrolysis-gas chromatograph/mass spectrometer using a Frontier Lab PY3030iD micro-furnace single-shot pyrolyzer connected to an Agilent Technologies 7890B gas chromatograph *via* a split-/splitless inlet port. An Agilent Technologies 7890B mass selective detector was combined with the gas chromatograph; the ionization energy (EI) was 70 eV and the scan range was 15–550 amu. 150 μg samples were pyrolyzed under helium atmosphere and inserted into the pyrolyzer *via* gravimetric fall; the temperature was 500 °C, except for measurements of **poly-1**, where the pyrolyzer temperature was set to 250 °C for an additional measurement. All evolved pyrolysis products were separated under a helium flow of 1 mL m^{-1} in an Ultra Allow+- 5 capillary column with a length of 30 m, inner diameter of 0.25 mm, and film thickness of 0.25 μm. First, the column was heated to 40 °C and held there for 2 min, then heated at a rate of 10 K min^{-1} up to 300 °C, where it was kept for 10 min. The GC injector was operated in a split mode of 1 : 300; the interface temperature was 300 °C. MS peak assignments were made using the NIST 14 MS library.

Cone calorimeter

Fire testing was conducted on an FTT cone calorimeter operating at a heat flux of 50 kW m^{-2} according to ISO 5660, simulating a developing fire.[39] Samples sized 100 mm × 100 mm × 4 mm were conditioned at 23 °C and 50% RH for at least 48 h, then measured at a distance of 35 mm from the cone heater, as a distance of 25 mm was not suitable for the large residues of the materials.[40]

GPC

GPC measurements were performed in DMF (+LiBr 1 g L^{-1}) with a PSS SecCurity system (Agilent Technologies 1260 Infinity). Sample injection was performed by a 1260-ALS autosampler (Waters) at 60 °C. SDV columns (PSS) with dimensions of 300 × 80 mm, 10 μm particle size, and pore sizes of 10 000, 1000, and 100 Å were employed. The IR 1260 RID detector and UV-vis 1260-VWD detector (Agilent) were used for detection. Calibration was achieved using poly(styrene) standards provided by Polymer Standards Service.

Elemental analysis

Elemental analysis was run on an Elementar Vario EL cube.

NMR

Nuclear magnetic resonance (NMR) analysis, ^{1}H, ^{31}P {H} and ^{13}C {H} NMR spectra were recorded with Bruker Avance spectrometers operating with 250, 300, 500 and 700 MHz frequencies in deuterated chloroform, deuterated dimethyl sulfoxide or deuterated *N*,*N*-dimethylformamide as a solvent. The calibration of the spectra was done against the solvent signal. The spectra were analyzed using MestReNova 9 from Mestrelab Research S.L.

4-Bromobutan-1-ol

The synthesis was done according to a literature procedure.[27] In a 1 L flask, THF (270 mL, 3.33 mol) was added to hydrobromic acid (48%, 180 g, 1.06 mol). The mixture was refluxed for two hours, transferred into an Erlenmeyer flask, and the reaction was neutralized by the addition of $NaHCO_3$ under strong CO_2 development. The aqueous solution was extracted with dichloromethane and the organic layers were combined and dried with Na_2SO_4. The solvent was removed at reduced pressure, yielding the product (47.3 g, 29%), which was used without further purification.

^{1}H NMR (250 MHz, $CDCl_3$): δ [ppm] = 4.01 (s, 1H), 3.69 (t, J = 6.4 Hz, 2H), 3.44 (t, J = 6.6 Hz, 2H), 2.05–1.79 (dd, J = 8.0, 6.6 Hz, 2H), 1.79–1.62 (dd, J = 8.5, 6.4 Hz, 2H).

4-Bromobutyl phosphorodichloridate (1a)

To a dried three-necked, 500 mL round bottom flask equipped with two 100 mL dropping funnels, 0.522 mol phosphoryl chloride (80.00 g, 47.62 mL, 521.78 mmol, 5.0 eq.) were added to ice-cooled, dry toluene (100 mL) under argon atmosphere. 4-bromobutan-1-ol (15.97 g, 9.51 mL, 104.36 mmol, 1.0 eq.) dissolved in dry toluene (50 mL) and pyridine (8.25 g, 8.42 mL, 104.36 mmol, 1.0 eq.) dissolved in dry toluene (50 mL) were added to the above flask dropwise, keeping the temperature at 0 °C. After stirring overnight at room temperature, pyridine hydrochloride was removed as a white solid by filtration. The filtrate containing the alkylene dichlorophosphate in toluene was concentrated at reduced pressure. 4-Bromobutyl phosphoro-dichloridate was obtained as a colourless liquid (yield: 21.6 g, 77%).

^{1}H NMR (300 MHz, 298 K, $CDCl_3$, δ/ppm): 4.43–3.34 (m, 2H), 3.49–3.43 (t, J = 5.8 Hz, 2H), 2.07–1.95 (m, 4H).

^{31}P{H} NMR (202 MHz, 298 K, $CDCl_3$, δ/ppm): 7.21.

4-Bromobutyldi(hex-5-en-1-yl) phosphate (1b)

To a dry three-necked, 500 mL round bottom flask fitted with a 250 mL dropping funnel, 5-hexen-1-ol (17.61 g, 21.11 mL, 175.29 mmol, 2.1 eq.) and pyridine (13.87 g, 14.15 mL, 175.29 mmol, 2.1 eq.) were added to dry toluene (100 mL) under an argon atmosphere. **1** (22.53 g, 83.47 mmol, 1.0 eq.) dissolved in dry toluene (100 mL) was added to the above flask dropwise at room temperature. After stirring overnight, pyridine hydrochloride was removed as a white solid by filtration. The organic solution was washed with sodium bicarbonate solution, 10% hydrochloric acid, and sodium chloride solution. The organic layer was dried over anhydrous sodium sulfate, filtered, and the solvent was removed at reduced pressure. 4-Bromobutyldi(hex-5-en-1-yl) phosphate was obtained as a yellow liquid (yield: 30.2 g, 88%).

^{1}H NMR (300 MHz, 298 K, $CDCl_3$, δ/ppm): 5.90–5.68 (m, 2H), 5.06–4.92 (m, 4H), 4.40–3.92 (m, 6H), 3.69–3.61 (t, J = 6.3 Hz, 2H), 3.48–3.40 (t, J = 6.3 Hz,2H), 2.21–2.05 (m, 4H), 2.05–1.74 (m, 4H), 1.74–1.59 (m, 4H), 1.53–1.41 (m, 4H).
^{31}P{H} NMR (202 MHz, 298 K, $CDCl_3$, δ/ppm): −0.71.

Di(hex-5-en-1-yl)(4-acetylthiobutyl)phosphate (1c)

To a dry one-necked, 500 mL round bottom flask, **2** (29.05 g, 73.11 mmol, 1.0 eq.) and potassium thioacetate (9.18 g, 80.42 mmol, 1.1 eq.) were dissolved in acetone (100 mL). After stirring overnight at room temperature, potassium bromide was removed as a white solid by filtration. Acetone was removed at reduced pressure and the residue was dissolved in toluene (100 mL). The mixture was washed with sodium bicarbonate solution, 10% hydrochloric acid and sodium chloride solution. The organic layer was dried over anhydrous sodium sulfate, filtered and the solvent was removed at reduced pressure to isolate *S*-(4-((bis(hex-5-en-1-yloxy)phosphoryl)oxy) butyl)ethanethioate (yield: 27.7 g, 96%).

^{1}H NMR (300 MHz, 298 K, $CDCl_3$, δ/ppm): 5.87–5.70 (m, 2H), 5.06–4.92 (m, 4H), 4.23–3.94(m, 6H), 3.92–2.82 (m, 4H), 2.32 (s, 3H), 2.13–2.02 (m, 4H) 1.79–1.63 (m, 8H), 1.54–1.42 (m 4H).

^{31}P{H} NMR (202 MHz, 298 K, $CDCl_3$, δ/ppm): −0.55.

Di(hex-5-en-1-yl)(4-mercaptobutyl)phosphate (1)

1c (26.78 g, 68.24 mmol, 1.0 eq.) was dissolved in dichloromethane (100 mL) in a dry one-necked, 500 mL round bottom flask. Then 1 M hydrazine in THF (102.36 mL, 102.36 mmol, 1.5 eq.) was added dropwise. After stirring overnight at room temperature, the mixture was washed with sodium bicarbonate solution, 10% hydrochloric acid and sodium chloride solution. The organic layer was dried over anhydrous sodium sulfate, filtered and concentrated *in vacuo*. The remaining liquid was purified by column chromatography (3 : 7 ethyl acetate/petroleum ether) to obtain an off-white oil (yield: 5.8 g, 24%).

^{1}H NMR (300 Hz, 298 K, $CDCl_3$, δ/ppm): 5.88–5.70 (m, 2H), 5.06–4.92 (m, 4H), 4.10–3.98 (m, 6H), 2.62–2.50 (m, 2H), 2.14–2.02 (m, 4H), 1.88–1.58 (m, 8H), 1.54–1.41 (m, 4H), 1.34 (t, J = 7.9 Hz, 1H).

^{31}P{H} NMR (202 MHz, 298 K, $CDCl_3$, δ/ppm): −0.68.

Poly-1

Poly-1 was prepared by a radical thiol–ene polyaddition. 33 g (94.2 mmol; 1.0 eq.) of the previously synthesized monomer **1** were dissolved in 230 mL toluene and added to a reactor fitted with a mechanical stirrer under an argon atmosphere. As a radical initiator, 1.4 g azobisisobutyronitrile (AIBN) (8.5 mmol; 0.1 eq.) was used. The solution was heated at 90 °C for

24 hours. The crude mixture was then concentrated and dried at reduced pressure until constant weight (yield: 32.5 g, 98.5%).

^{1}H NMR (300 Hz, 298 K, $CDCl_3$, δ/ppm): 5.88–5.70 (m, 2H), 5.06–4.92 (m, 4H), 4.10–3.98 (m, 6H), 2.62–2.50 (m, 4H), 2.14–2.02 (m, 4H), 1.88–1.58 (m, 8H), 1.54–1.41 (m, 4H).

^{31}P{H} NMR (202 MHz, 298 K, $CDCl_3$, δ/ppm): −0.70.

Poly-2

The synthesis was done according to a literature procedure.[11]

Poly-1 for kinetic studies

In a 25 mL Schlenk tube, **1** (405 mg, 1.16 mmol) was dissolved in toluene (2.7 mL) under an argon atmosphere. AIBN (0.03, 0.06, or 0.09 eq.) was added to the Schlenk tube and the mixture was heated to 70 °C or 90 °C. After specific reaction times, samples (each 0.2 mL) were taken and terminated in air for the analysis of the polymerization kinetics. The crude product was dried *in vacuo* and analyzed by ^{1}H, ^{31}P NMR, and GPC.

^{1}H NMR (300 Hz, 298 K, $CDCl_3$, δ/ppm): 5.88–5.70 (m, 2H), 5.06–4.92 (m, 4H), 4.10–3.98 (m, 6H), 2.62–2.50 (m, 4H), 2.14–2.02 (m, 4H), 1.88–1.58 (m, 8H), 1.54–1.41 (m, 4H).

^{31}P{H} NMR (202 MHz, 298 K, $CDCl_3$, δ/ppm): −0.70.

Epoxy preparation

All epoxy resins were prepared using bisphenol A diglycidylether (DGEBA) (Araldite MY740, Bodo Möller Chemie GmbH, Offenbach am Main, Germany) as the epoxide agent and 2,2′-dimethyl-4,4′-methylene-bis-(cyclohexylamine) (DMC) (Sigma Aldrich Co. LLC/Merck KgaA, Darmstadt, Germany) as the amine hardener. The materials were mixed, poured into aluminum molds of desired dimensions, then hardened at 150 °C for 3 h. The flame retarded epoxy resins were produced in the same manner, except 10 wt% of the mixture was replaced with the respective flame retardant.

Author contributions

The manuscript was written through contributions of all authors. All authors have given approval to the final version of the manuscript.

Conflicts of interest

There are no conflicts to declare.

Acknowledgements

The authors thank the Deutsche Forschungsgemeinschaft (DFG WU 750/8-1; SCHA 730/15-1) for funding. Jens C. Markwart is the recipient of a fellowship through funding of the Excellence Initiative (DFG/GSC 266) in the context of the graduate school of excellence "MAINZ" (Materials Science in Mainz). F. R. Wurm and Jens C. Markwart thank Prof. Dr. Katharina Landfester (MPI-P, Germany) for support. Alexander Battig thanks Dr. Katharina Kebelmann and Patrick Klack for their support with Py-GC/MS and the cone calorimeter. Open Access funding provided by the Max Planck Society.

References

1 J. Liu, W. Huang, Y. Pang and D. Yan, *Chem. Soc. Rev.*, 2015, **44**, 3942–3953.
2 M. D. Lechner, K. Gehrke and E. H. Nordmeier, *Makromolekulare Chemie: Ein Lehrbuch für Chemiker, Physiker, Materialwissenschaftler und Verfahrenstechniker*, Springer, Berlin Heidelberg, 2014.
3 B. I. Voit and A. Lederer, *Chem. Rev.*, 2009, **109**, 5924–5973.
4 B. Schartel and J. H. Wendorff, *Polym. Eng. Sci.*, 1999, **39**, 128–151.
5 K. Täuber, F. Marsico, F. R. Wurm and B. Schartel, *Polym. Chem.*, 2014, **5**, 7042–7053.
6 B. Perret, B. Schartel, K. Stöß, M. Ciesielski, J. Diederichs, M. Döring, J. Krämer and V. Altstädt, *Eur. Polym. J.*, 2011, **47**, 1081–1089.
7 B. Perret, B. Schartel, K. Stöß, M. Ciesielski, J. Diederichs, M. Döring, J. Krämer and V. Altstädt, *Macromol. Mater. Eng.*, 2011, **296**, 14–30.
8 C. R. Yates and W. Hayes, *Eur. Polym. J.*, 2004, **40**, 1257–1281.
9 S. Penczek, K. Kaluzynski and J. Pretula, *J. Appl. Polym. Sci.*, 2007, **105**, 246–254.
10 J. Liu, W. Huang, Y. Pang, X. Zhu, Y. Zhou and D. Yan, *Biomacromolecules*, 2010, **11**, 1564–1570.
11 A. Battig, J. C. Markwart, F. R. Wurm and B. Schartel, *Polym. Chem.*, 2019, **10**, 4346–4358.
12 J. Khandare, M. Calderón, N. M. Dagia and R. Haag, *Chem. Soc. Rev.*, 2012, **41**, 2824–2848.
13 Y. Zhou, W. Huang, J. Liu, X. Zhu and D. Yan, *Adv. Mater.*, 2010, **22**, 4567–4590.
14 F. Marsico, A. Turshatov, R. Peköz, Y. Avlasevich, M. Wagner, K. Weber, D. Donadio, K. Landfester, S. Baluschev and F. R. Wurm, *J. Am. Chem. Soc.*, 2014, **136**, 11057–11064.
15 M. M. Velencoso, A. Battig, J. C. Markwart, B. Schartel and F. R. Wurm, *Angew. Chem., Int. Ed.*, 2018, **57**, 17.
16 P. Wen, X. Wang, W. Xing, X. Feng, B. Yu, Y. Shi, G. Tang, L. Song, Y. Hu and R. K. K. Yuen, *Ind. Eng. Chem. Res.*, 2013, **52**, 17015–17022.
17 J. Li, C. Ke, L. Xu and Y. Wang, *Polym. Degrad. Stab.*, 2012, **97**, 1107–1113.
18 K.-C. Cheng, C.-C. Wang, J.-l. Ruan, C.-H. Wu and C.-W. Li, *Polym. Adv. Technol.*, 2018, **29**, 2529–2536.
19 M. Rakotomalala, S. Wagner and M. Döring, *Materials*, 2010, **3**, 4300.
20 K. H. Pawlowski and B. Schartel, *Polym. Int.*, 2007, **56**, 1404–1414.

21 B. Perret, K. H. Pawlowski and B. Schartel, *J. Therm. Anal. Calorim.*, 2009, **97**, 949.
22 C. Gao and D. Yan, *Prog. Polym. Sci.*, 2004, **29**, 183–275.
23 P. J. Flory, *J. Am. Chem. Soc.*, 1952, **74**, 2718–2723.
24 D. Yan, C. Gao and H. Frey, *Hyperbranched Polymers: Synthesis, Properties, and Applications*, Wiley, 2011.
25 P. J. Flory, *J. Am. Chem. Soc.*, 1941, **63**, 3083–3090.
26 C. Walling, *J. Am. Chem. Soc.*, 1945, **65**, 441–447.
27 H. Tan, H. Liu, X. Chen, H. Chen and S. Qiu, *Org. Biomol. Chem.*, 2015, **13**, 9977–9983.
28 J. C. Markwart and F. R. Wurm, *Tetrahedron*, 2018, **74**, 7426–7430.
29 M. Ciesielski, A. Schäfer and M. Döring, *Polym. Adv. Technol.*, 2008, **19**, 507–515.
30 B. Schartel, C. A. Wilkie and G. Camino, *J. Fire Sci.*, 2016, **34**, 447–467.
31 J. C. Markwart, A. Battig, L. Zimmermann, M. Wagner, J. Fischer, B. Schartel and F. R. Wurm, *ACS Appl. Polym. Mater.*, 2019, **1**, 1118–1128.
32 L.-H. Lee, *J. Polym. Sci., Part A: Gen. Pap.*, 1965, **3**, 859–882.
33 D. P. Bishop and D. A. Smith, *J. Appl. Polym. Sci.*, 1970, **14**, 205–223.
34 M. Ciesielski, B. Burk, C. Heinzmann and M. Döring, in *Novel Fire Retardant Polymers and Composite Materials*, ed. D.-Y. Wang, Woodhead Publishing, 2017, pp. 3–51, DOI: 10.1016/B978-0-08-100136-3.00002-9.
35 B. Schartel, B. Perret, B. Dittrich, M. Ciesielski, J. Krämer, P. Müller, V. Altstädt, L. Zang and M. Döring, *Macromol. Mater. Eng.*, 2016, **301**, 9–35.
36 B. Perret, K. Pawlowski and B. Schartel, *J. Therm. Anal. Calorim.*, 2009, **97**, 949–958.
37 S. Brehme, B. Schartel, J. Goebbels, O. Fischer, D. Pospiech, Y. Bykov and M. Döring, *Polym. Degrad. Stab.*, 2011, **96**, 875–884.
38 R. V. Petrella, *J. Fire Sci.*, 1994, **12**, 14–43.
39 B. Schartel and T. R. Hull, *Fire Mater.*, 2007, **31**, 327–354.
40 B. Schartel, M. Bartholmai and U. Knoll, *Polym. Degrad. Stab.*, 2005, **88**, 540–547.